To: Hydrology and Earth Systems Sciences Discussion

Re: Interactive comment on "A review of applications of satellite SAR, optical, altimetry and DEM data for surface water modelling, mapping and parameter estimation"
by Z. N. Musa et al.

Dear Editor

Please find, in the submission section of the Authors, the new version of the manuscript " *"A review of applications of satellite SAR, optical, altimetry and DEM data for surface water modelling, mapping and parameter estimation"* (hess-2015-165) which we are submitting following the comments received from you and the reviewers. We have amended the manuscript with all requested changes by the reviewers.

We would like to thank the editor and the reviewers for taking time in reading and suggesting modifications to the paper. With received suggestions we have improved the manuscript.

Please find below this letter the responses to your comments with reference to issues raised by reviewer number one, and the marked up version of the manuscript showing all changes made within the text.

As per reviewers suggestion we made several modifications to the manuscript; added details to all the sections; restructured the manuscript; included two more figures and a table describing commonly used satellite data in hydrology for surface water applications. All the modifications were made by carefully looking at the questions, researching more literature and updating the information included in the manuscript. Consequently, we have added all the cited literature in the new version of the manuscript.

We have submitted a manuscript with highlighted changed areas so that the new additions and modifications can be compared with the initial text.

Thank you very much for your kind consideration of this resubmitted version of our manuscript.

Sincerely yours,
Zahrah N. Musa
(On behalf of the authors of the manuscript)

Manuscript modification based on Reviewer #1 comment no 3

The responses to the individual comments of reviewer#1 are detailed below.
(Note: Reviewer comments are in italic, authors' responses are in normal text)

Comment3: Some of the topics covered in the Yan review that are not mentioned here are: The use of the new high resolution SARs for flood detection (e.g. CSK, TerraSAR-X, RADARSAT-2, PALSAR), including mapping of flooding in urban as well as rural areas. The CSK constellation satellites can have a revisit interval of 12 hours for a flood, which is sufficiently frequent to capture floods in medium-sized catchments. Also, there is no mention here of the Sentinel-1 constellation (the first of which is already working), which will give high resolution images in near real-time (making them suitable for flood forecasting operations), on an almost daily basis in Europe. The methods used to derive flood extent data from SAR images are also not considered e.g. Martinis et al., 2009, 2011).

Authors Answer: based on the comments above, the manuscript has been modified to include the following:

1. Under future direction in satellite applications for hydrology, we discuss the available satellite data (such as TERRASAR-X) that provide an improvement in the DEM quality. This explanation is given as follows:

   With better SAR missions such as TerraSAR-X- TanDEM-X formation, DEM data with good vertical accuracy are now available for better hydraulic flood modelling. TanDEM-X has 12.5m spatial resolution and produces less than 2m vertical accuracy (DLR, 2015). Although made for polar ice change estimation and monitoring, the high spatial coverage of Cryosat-2 is also being exploited for near-shore mapping and inland water monitoring; all evaluations have produced good results (Villladsen, Andersen, & Stenseng, 2014). Cryosat-2 has a drifting orbit and therefore (unlike all the other satellites) has little repetitive data (since repeat cycle is 369 days) but high spatial density coverage, which makes it good for hydraulic modelling. With successful use of Cryosat-2 data to obtain river water levels and topography, the use of drifting orbits is being proposed as more suitable for river water surface topography mapping, derivation of river profiles and building of pseudo time series (Bercher, et al., 2014).

   Other satellite products that improve the accuracy of satellite data based research in hydrology include: Cosmo-SkyMed from the Italian Space Agency, RadarSat2 from the Canadian Space Agency, and Sentinel-1 from ESA (Schumann, et al., 2015). Others are Global Change Observation mission-water (GCOM-W) from Japan Space Agency (JAXA), Global Precipitation Measurement (GPM) from JAXA /USA, Soil Moisture Active Passive (SMAP) from USA.

   To improve quality of satellite SAR and topographic data, new satellite missions with higher precision instruments are being planned. One of such missions is the Sentinel constellation that will consist of seven satellites; two of which (Sentinel 3 and 6) are especially dedicated to hydrological purposes. Sentinel 1 is already in orbit and undergoing calibration; it has a C-band SAR instrument to continue present C-band data provision. Sentinel 3 is planned to provide fast data for flood emergencies, therefore it has three instruments one of which is a dual-frequency (Ku and C band) advanced Synthetic Aperture Radar Altimeter (SRAL) that will provide accurate topographic data of oceans, ice sheets, sea ice, rivers and lakes (ESA, 2015). Sentinel 6, which will compliment the Sentinel 3 data, will carry on board a high precision radar altimeter. RADARSAT constellation, a new Low Earth Orbit (LEO) C-band SAR mission is under development by the Canadian space Agency (CSA). The constellation which will have several operating modes will provide interferometric SAR data that can be used for wetlands and coastal change mapping, flood disaster warning and response with resolutions 3, 5, 16, 30, 50 and 100m (Canadian Space Agency (CSA), 2015).

   <u>References included in the text</u>

1. Schumann, G. J.-P., Neal, J., Voisin, N., Andreadis, K., Pappenberger, F., Phanthuwongpakdee, N., and Bates, P. (2013). A first large-scale flood inundation forecasting model. Water Resources Research, 49, 6248–6257. Doi:10.1002/wrcr.20521, 2013

2. Villladsen, H., Andersen, O., & Stenseng, L. (2014). Annual cycle in lakes and rivers from cryosat-2 altimetry - the brahmaputra river. International Geoscience and Remote Sensing Symposium (IGARSS) (pp. 894-897). 13-18 July 2014. Quebec, Canada: IEEE. Doi:978-1-4799-5775-0/14

3. Bercher, N., Calmant, S., Picot, N., Seyler, F., & Fleury, S. (2014). Evaluation of Cryosat-2 measurements for the monitoring of large river water levels. Retrieved from: Along-Track.com: http://chronos.altihydrolab.fr/2012-09-23%20Venice%20ESA%2020%20years%20of%20progress%20in%20altimetry/Bercher.2012b%20(Venice%20Paper)%20CryoSat-2%20hydro.pdf (Last access 25-06-2015)

4. ESA. (2015). Sentinel 3. Retrieved from Copernicus, observing the Earth: http://www.esa.int/Our_Activities/Observing_the_Earth/Copernicus/Sentinel-3 (Last access June 15, 2015)

5. Canadian Space Agency (CSA). (2015). RADARSAT Constellation. Retrieved from RADARSAT constellation: http://www.asc-csa.gc.ca/eng/satellites/radarsat/ (Last access June 23, 2015)

2. The methods used to derive flood extent from SAR data are also included within the text with examples of applications also given. The additional text reads as follows:

SAR data are useful for flood extent measurements even in cloud covered areas, and are therefore often used to make flood maps (e.g. Schumann, et al., 2007; Horritt, 2006; Di Baldassarre, et al., 2009; Vermeulen, et al., 2005; Mason, et al., 2007; Long et al., 2014). The variation of radar backscatter from different targets enables flood extent mapping. Several methods have been used to delineate the flooding extent from SAR data; e.g. utilization of multi-polarized Advanced SAR images, application of a statistical active control model, multi-temporal image enhancement and differencing, histogram thresholding/ clustering, radiometric thresholding, pixel-based segmentation, use of artificial neural networks, etc (Long et al,. 2014) . Multi-temporal image flood mapping involves acquiring flooding and non-flood images of the same area and combing them to get an image which indicates change by colours appearing in the image. A modification of the multi-temporal technique introduces an index that shows the changing areas (Skakun, 2010). Sarhadi et al., (2012) applied satellite stereoscopic images of Cartosat-1 to delineate flood hazard maps; the method used Rational Polynomial Coefficients to extract a high resolution DTM and detailed parameterization of the channel in Halilrud basin and Jiroft city in south-eastern Iran.

Segmentation threshold algorithms are used to delineate flood extents after a threshold has been manually chosen. Flood extent maps were created over four years of seasonal flooding in the Chobe floodplain, Namibia (Long et al,. 2014). 11 scenes of SAR data were enhanced using adaptive Gamma filtering (to remove speckles), and difference images created by subtracting from the reference non flood season image. The histograms of the difference images were then used to create thresholds separating flooded and non-flooded areas. The threshold for flooded areas was determined by subtracting the standard deviation multiplied by a coefficient Kf from the mean pixel value. For flooding under vegetated areas, the threshold was determined adding the standard deviation multiplied by a coefficient Kfv to the mean pixel value. The flood maps were then created using segmentation clustering in ENVI. Segmentation based on self-organizing Kohonen's maps (SOM) neural networks was used by Skakun (2010) to map flooding from five rivers in China, India, Hungary, Ukraine, Laos and Thailand. Training and testing of the neural networks were based on ground-truth data which enabled classification of water and dry land pixels. SOM produces a low dimensional representation of the input space that still preserves the topological properties of the input space. The method enabled automatic discovery of statistically salient features of pattern vectors, clustering and classification of new patterns. The resulting flood maps show an 85-95% classification rate compared with independent testing data; showing the applicability of the method for emergency flood mapping.

Interferometric phase difference between two SAR images is called the interferogram and includes signatures from topography, noise, displacement, atmospheric effects and baseline error. The advantage of phase changes in SAR interferometer data (INSAR) enables detection of change in the Earths land-use and land cover. This characteristic is very useful for identification of flooded areas over wetlands as used by (Dellepiane et al., 2004). The method, based on fuzzy connectivity concepts, automatically selected the coastline from two InSAR imagery using the coherence of the two images.

References included in the text

1. Vermeulen, C. J. M., Barneveld, H. J., Huizinga, H. J. & Havinga, F. J., 2005. Data-assimilation in flood forecasting using time series and satellite data. Tromso, ACTIF/Floodman/FloodRelief

2. Schumann, G. et al., 2007. Deriving distributed roughness values from satellite radar data for flood inundation modelling. Journal of Hydrology, 344(1-2), p. 96–111.

3. Di Baldassarre, G., Schumann, G. & Bates, P. D., 2009. A technique for the calibration of hydraulic models using uncertain satellite observations of flood extent. Journal of Hydrology, 367(3-4), p. 276–282

4. Horritt, M. S., 2006. A methodology for the validation of uncertain flood inundation models. Journal of Hydrology, 326(1-4), p. 153–165.

5. Mason, D. C., Horritt, M. S., Dall'Amico, J. T., & Scott, T. R. (2007). Improving River Flood Extent Delineation From Synthetic Aperture Radar Using Airborne Laser Altimetry. IEEE Transactions on Geoscience and Remote Sensing and(0196-2892), 3932 - 3943. doi:10.1109/TGRS.2007.901032

6. Long, S., Fatoyinbo, T., & Policelli, F. (2014). Flood extent mapping for Namibia using change detection and thresholding with SAR. Environmental Research Letters, 9(035002). doi:10.1088/1748-9326/9/3/035002

7. Sarhadi, A., Soltani, S., & Modarres, R. (2012). Probabilistic flood inundation mapping of ungauged rivers: Linking GIS techniques and frequency analysis. Journal of Hydrology, 458-459, 68-86. doi:10.1016/j.jhydrol.2012.06.039

8. Dellepiane, S., de Laurentiis, R., & Giordano, F. (2004). Coastline Extraction from SAR Images and a Method for the Evaluation of the Coastline Precision. Pattern Recognition Letters, 25, 1461–1470.

A review of applications of satellite SAR, Optical, Altimetry and DEM data for surface water modelling, mapping and parameter estimation

Z. N. Musa[1], I. Popescu[1], A. Mynett [1,2]

 [1]{ UNESCO-IHE Institute for Water Education, Delft, The Netherlands }

[2]{ Department of Civil Engineering, Technical University Delft, The Netherlands }

Correspondence to: z.musa@unesco-ihe.org

Abstract

Hydrological data collection requires deployment of physical infrastructure like rain gauges, water level gauges, as well as use of expensive equipment like echo sounders. Many countries around the world have recorded a decrease in deployment of physical infrastructure for hydrological measurements; developing countries especially have less of this infrastructure and where they exist, they are poorly maintained. Satellite remote sensing can bridge this gap, and has been applied by hydrologists over the years, with the earliest applications in water body and flood mapping. With the availability of more optical satellites with relatively low temporal resolutions globally, satellite data is commonly used for: mapping of water bodies, testing of inundation models, precipitation monitoring, and mapping of flood extent. Use of satellite data to estimate hydrological parameters continues to increase due to use of better sensors, improvement in knowledge of/ and utilization of satellite data, and expansion of research topics. A review of applications of satellite remote sensing in surface water modelling, mapping and estimation is presented, and its limitations for surface water applications are also discussed.

1. Introduction

Hydrological data collection still remains a difficult task nowadays due to <mark>non-availability</mark> of measurement devices, inaccessibility of the terrain and limitations of space/time (Quin et al, 2010; Pereira-Cardenal, et al., 2011). A good alternative to overcome these difficulties is use of satellite remote sensing, which can give a synoptic view of target areas (figure 1), measure target surface changes and therefore provide information needed for hydrological studies, river basin management, water hazard/ disaster monitoring/prevention and water management, etc. Through the science of

remote sensing, information about an object can be obtained without coming in direct contact with it (Lillesand, et al., 2004). This capability works by measuring electromagnetic energy reflected or radiated from objects on the earth's surface (figure 1), in such a way that the difference in reflectivity of objects enables recognition/detection and isolation of each type/class (figure 2).

Remotely sensed data are of two types depending on the main source of energy. Passive remote sensing depends on natural energy from the sun. Active remote sensing uses controlled energy sources from instruments beaming sections of the electromagnetic spectrum. Imagery obtained via instruments that measure reflectance from the sun, are known as optical imagery. Optical imagery from satellites is therefore acquired during the day since it depends on the reflections of sunlight from objects on the earth surface in the absence of cloud cover. Depending on the mission specifications satellites are placed on different kinds of orbits around the earth. The orbits include: Low Earth Orbit (LEO), Medium Earth Orbit (MEO), and Geo-Synchronous orbits (GSO); variations of these classes of orbits are the polar orbit, the Geostationary orbits, the Molneya orbit and the sun-synchronous orbit. Most optical satellites used for hydrological applications are in near earth orbits and are therefore able to provide detailed data at high ground (e.g. figure 1); although the best resolution data are usually not freely available and expensive to obtain. Due to this detailed resolution, optical satellite imagery is used for inundation mapping, drainage mapping, disaster monitoring, land-use/land cover change analysis etc (Owe, et al., 2001).

Active remote sensing can provide data as imagery (e.g. radar), and in the form of pulse measurements (e.g. altimeters and scatterometers). Radar is an active source of remote sensing data which acquires data via instruments that emit radar signal towards the object of interest and measure the reflected energy from the object. Radar can penetrate cloud cover and can be acquired at any time independent of availability of sunlight. The penetration characteristic of the SAR satellites enables measurement of soil moisture in bare areas, making it useful for land-use and land cover studies as well as earth observation and monitoring (Owe, et al., 2001). SAR is a side-looking instrument that sends out signals inclined at an angle. For water bodies the reflectivity of SAR waves is spectacular giving a very low radar return and very dark images. However when there are surrounding or emergent vegetation, wind, turbulence etc, there can be significant backscatter; which affects the accuracy of information obtained from the radar measurements (Smith, 1997).

Satellite remote sensing has been applied in hydrology for many years. Table 1 shows some satellite missions and sensors used for hydrological studies and the application areas. A review by Smith, (1997) shows that the earliest hydrological applications were in water body and flood mapping; the review includes many examples of inundation maps developed from satellite imagery. Owe, et al.,

(2001) also compiled papers presented at a conference on applications of remote sensing in many aspects of hydrology. Beyond mapping, satellite data in the form of imagery, DEM, altimetry data, etc, can be used as hydraulic model input forcing factors or to constrain model data during calibration/validation/verification (Pereira-Cardenal, et al., 2011). Satellite based estimates of river flow, river width, water levels and flooding extent are used for model calibration/validation/verification. Choice of suitable observed data can introduce subjectivity in the modelling process and subsequently increase uncertainty. Consequently, satellite data used to benchmark the model output accuracy can influence model calibration and validation (Stephens, et al., 2012). A review of types of satellite data used for flood modelling by Yan, et al., (2015) discusses satellite data accuracy and methods used for error reduction.

The main scope of this review is to present literature findings about application of satellite remote sensing in surface water modelling, mapping and parameter estimation. The review limits itself to water flowing within channels and coastal areas, and therefore excludes applications of satellite remote sensing for soil moisture measurement, rainfall estimation, rainfall/run off modelling and its associated routing estimations.

The paper is structured into two main parts. The first gives an overview of applications of SAR, Optical, Altimetry and DEM data for estimation of surface water parameters, modelling and mapping. The second part discusses the limitations of utilizing satellite derived data in surface water applications and the future directions aimed to fill the gaps. The review ends with a conclusion.

2. Overview of Satellite data applications for surface water studies

1. SAR data applications

SAR data are useful for flood extent measurements even in cloud covered areas, and are therefore often used to make flood maps (e.g. Schumann, et al., 2007; Horritt, 2006; Di Baldassarre, et al., 2009; Vermeulen, et al., 2005; Mason, et al., 2007; Long et al., 2014). The variation of radar backscatter from different targets enables flood extent mapping. Several methods have been used to delineate the flooding extent from SAR data; e.g. utilization of multi-polarized Advanced SAR images, application of a statistical active control model, multi-temporal image enhancement and differencing, histogram thresholding/ clustering, radiometric thresholding, pixel-based segmentation, use of artificial neural networks, etc (Long et al,. 2014) . Multi-temporal image flood mapping involves acquiring flooding and non-flood images of the same area and combing them to get an

image which indicates change by colours appearing in the image. A modification of the multi-temporal technique introduces an index that shows the changing areas (Skakun, 2010). Sarhadi et al., (2012) applied satellite stereoscopic images of Cartosat-1 to delineate flood hazard maps; the method used Rational Polynomial Coefficients to extract a high resolution DTM and detailed parameterization of the channel in Halilrud basin and Jiroft city in south-eastern Iran.

Segmentation threshold algorithms are used to delineate flood extents after a threshold has been manually chosen. Flood extent maps were created over four years of seasonal flooding in the Chobe floodplain, Namibia (Long et al,. 2014). 11 scenes of SAR data were enhanced using adaptive Gamma filtering (to remove speckles), and difference images created by subtracting from the reference non flood season image. The histograms of the difference images were then used to create thresholds separating flooded and non-flooded areas. The threshold for flooded areas was determined by subtracting the standard deviation multiplied by a coefficient K_f from the mean pixel value. For flooding under vegetated areas, the threshold was determined adding the standard deviation multiplied by a coefficient K_{fv} to the mean pixel value. The flood maps were then created using segmentation clustering in ENVI. Segmentation based on self-organizing Kohonen's maps (SOM) neural networks was used by Skakun (2010) to map flooding from five rivers in China, India, Hungary, Ukraine, Laos and Thailand. Training and testing of the neural networks were based on ground-truth data which enabled classification of water and dry land pixels. SOM produces a low dimensional representation of the input space that still preserves the topological properties of the input space. The method enabled automatic discovery of statistically salient features of pattern vectors, clustering and classification of new patterns. The resulting flood maps show an 85-95% classification rate compared with independent testing data; showing the applicability of the method for emergency flood mapping.

Interferometric phase difference between two SAR images is called the interferogram and includes signatures from topography, noise, displacement, atmospheric effects and baseline error. The advantage of phase changes in SAR interferometer data (INSAR) enables detection of change in the Earths land-use and land cover. This characteristic is very useful for identification of flooded areas over wetlands as used by (Dellepiane et al., 2004). The method, based on fuzzy connectivity concepts, automatically selected the coastline from two InSAR imagery using the coherence of the two images.

InSAR has been used to calculate the changes in water levels using satellite altimetry data for calibration (Kim, et al., 2009; Jung, et al., 2010). To obtain the displacement phase used to obtain the change in water height, all other signals are removed. The interferogram data gives the relative water

level change between two locations. Where there is measured water level data (within acceptable radius) the relative water level change can be converted into the absolute water level change. Jung el al., (2010) used interferometric SAR data from JERS-1 to study change in water levels for the Amazon and Congo rivers. The data were acquired for the low flow and high flow seasons and processed using the 'two pass' method which includes flat earth phase removal and interferometric phase removal. Flooded vegetation, non-flooded areas and open water were differentiated based on backscatter 'noise floor' and 'mean interferometric coherence' of flooded and non-flooded areas. The temporal variation in water level dh/dt was obtained by converting the phase changes in imagery to water level referenced to the WGS84 datum using altimeter measurements from Topex/Poseidon. Using dh/dt to characterize the Amazon floodplain showed increasing dh/dt from upstream to downstream within a complex pattern of interconnected channels with distinct boundaries and varying dh/dt. The Congo River characterization of dh/dt showed a uniformity and limited connectivity between the river and the adjoining wetlands. Schumann et al., (2007) used Envisat ASAR data to identify spatial clusters of channel roughness in order to calibrate a HEC-RAS model of Alzette river flooding. ERS SAR data of the same event and an aerial photo of an earlier event were used for validation of the calibrated model and overall model performance was compared to measured high water marks at seven points during the flood event. The mean cross sectional water levels used for model evaluation were estimated from the intersection of ASAR flood extent boundaries with LIDAR DEM. At each cross section, ranges of channel roughness values are run in a Monte Carlo simulation and the CDF's of the values are generated; these CDF's are compared with a CDF of uniformly distributed model (where model functioning is same over the entire parameter space). The deviation of the individual CDF's from the CDF of uniform distribution give the measure of the parameter sensitivity, the sum of which show the local functioning of the model at that cross section. CDF's with similar error characteristics are grouped into clusters using k-mean clustering. The results showed that two clusters of roughness values are enough to measure the parameter sensitivity.

To utilise SAR data for flood depth estimation, methods have been developed that derive flood heights from flood extent data. The methods used combine SAR data with elevation data sources like DEMs, altimetry, and TINs. Mason, et al., (2007) and Schumann, et al., (2006), estimated the mean cross sectional water levels used for model evaluation from the intersection of SAR flood extent boundaries with LIDAR DEM. Schumann, et al., (2006) used linear regression and an elevation based model (REFIX) to convert SAR flood extent to heights and derived the flood water depth. Assuming a horizontal water height at cross sections, the water levels on the left and right banks

were taken and used to subtract the floodplain DEM values to get the water height. The flood water line was then extracted using the regression equation: $H = a.d + b$, where a= slope of the regression line, d= downstream water distance, b= intercept. Using the cross sections as break lines and the flood water heights extracted, a TIN of the water heights at each cross section was produced. The flood water depth was derived by subtracting the DEM at the cross sectional interception points from the flood water height TIN. The result showed an RMSE of 18cm for a channel with no hydraulic structures and 31cm for a channel with many hydraulic structures and changes in slope. The study recommends that nonlinear regression/ piece wise regression can be used in the case of sudden changes in slope (due to hydraulic structures etc) that cause the channel geometry to change.

Altimetry data from ENVISAT was combined with INSAR data from PALSAR and Radarsat-1 to compute absolute water level changes over the wetlands of Louisiana (Kim et al., 2009). Two pass INSAR method was used to check the two SAR images acquired at different times for phase differences. The ENVISAT altimetry data was used as the reference absolute water level change dh_0/dt to compute the all the changes in water level over the domain. The results obtained for water level changes showed better comparison with the wetland gauge than with the channel gauge which had many levees interrupting the flow. Westahoff, et al., (2010) mapped probabilistic flood extents from SAR data by using the amount of backscatter and local incidence angles to create histograms that distinguish between wet and dry areas. The histograms were used to calculate the probability of flooding of every pixel.

Satellite data is used to calibrate hydrologic models especially in un-gauged catchments (Vermeulen et al, 2005; Sun, et al., 2009). Calibration of flood inundation models can be done using several model parameters, but the most sensitive parameter that shows a direct relation with water stage and therefore flooding extent and timing is the channel roughness (Schumann et al., 2007). Woldemicheal et al., (2010) showed that for braided rivers where the hydraulic radius is obtained from indirect sources like satellite data, Manning's roughness coefficients can be used to minimize computed water level outliers. Roughness coefficient values to be used for calibration can be determined via flood modelling where the measured data are available.

Satellite based maps of flood extent have been used to calibrate flood inundation models either based on single or multiple flood events (Di Baldassarre, et al., 2009). Horritt (2006) calibrated and validated a model of uncertain flood inundation extent for the Severn River using observed flooded extent mapped from satellite imagery. Model accuracy was checked using reliability diagrams, and model precision was checked using an entropy-like measure which computes the level of uncertainty in the flood inundation map. The ensemble model outputs were compared with ERS and Radarsat

data for calibration using the measure of fit. The results showed that the mapped flood extent produced only a modest reduction in the uncertainty of model predictions because the timing of satellite passes did not coincide with the flood event. Di Baldassarre, et al., (2009) showed that satellite flood imagery acquired during an event can be reliable for flood mapping. They used imagery of a single event covered by two satellite passes captured almost at the same time to develop a method to calibrate flood inundation models based on 'possible' inundation extents from the two imageries. Hydrodynamic flood model extents were compared with the satellite flood extent maps in order to calibrate the floodplain frictional parameters and determine the best satellite resolution for flood extent mapping. In spite of their different resolutions the result showed that both satellite imageries could be used for model calibration, but different frictional values have to be used in the model.

For un-gauged basins where hydrological data is inaccessible, satellite measurement of river width can be used for hydrological model calibration (Schumann, et al., 2013; Sun, et al., 2009). River width can be estimated from several sources of satellite data; making it more readily available than discharge or water level. Sun, et al., (2009) used measured river width from satellite SAR imagery to calibrate HYMOD hydrological model. The model calibration based on river width gave 88.24% Nash coefficient, with a larger error during low flow than high flow periods; implying its usefulness for flood discharge calculations. From the results, braided rivers showed lower errors for good Q-W relations from satellites. However, a small error in width measurement can lead to a large error in discharge estimation as the discharge variability was much larger than the width variability. Sun, et al., (2010) used the GLUE methodology to reduce this uncertainty in calibration of river width -to-discharge estimation with the HYMOD hydrological model. From 50000 samples of the parameter sets, 151 (Likelihood=RMSE values) succeeded as behavioural sets to be used in the model to simulate the measured satellite river widths. River discharge simulated with the successful parameters (Likelihood = Nash-Sutcliffe efficiency) gave good discharge simulation with a correlation $R^2 = 0.92$.

Model use in forecasting is affected by the propagation of the input uncertainties which make it less accurate. Data assimilation can be used to reduce the accumulation of errors in hydraulic models. Assimilation combines model predictions with observations and quantifies the errors between them in order to determine the optimal model and improve future forecasts (Mcmillan, et al., 2013). Types of assimilation techniques include Kalman filter (and its variations), particle filter and variational technique. Particle filter assimilation is a bayesian learning system which accounts for input data uncertainty propagation by selecting suitable input data from randomly generated ones without

assuming any particular distribution of their PDF (Noh, et al., 2011). Particle filter technique was used in studies like Matgen, et al., (2010), Giustarini, et al., (2011) where input data are in form of ensemble flow outputs of a hydrological model. In Giustarini, et al., (2011) to assimilate water levels derived from two SAR images of flooding in the Alzette River into a hydraulic model, 64 upstream flows were generated from an ensemble hydrologic model and used as the upstream boundary conditions. The most commonly used data assimilation technique however, is the Kalman filter which is a state-space filtering method which assumes a Gaussian distribution of errors. Vermeulen et al., (2005) used SAR derived flood maps and time series data to make flood forecasting more accurate through data assimilation. The assimilation process based on kalman filtering technique used adaptation factors to multiply the original model output and adaptation factor in order to generate a new parameter value. The process included calculation of water levels/discharge on the Rhine River by combining hydrologic modelling of the sub-basins and hydraulic modelling using downstream measured data. Data assimilation was done using measured water levels to determine the roughness coefficients which calibrate the calculated water levels. The model output water levels were compared with water levels derived from flood maps but because the natural flow of the channel or floodplain has been modified, good results were only obtained when the geo-referencing of the map is deliberately shifted or the flooding extent is exaggerated by adding some random noise over a large area of 7-12km. Barneveld, et al., (2008) applied the same method and models for flood forecasting on the Rhine River and produced good results of 10 day forecasts; therefore assimilating data for natural catchments results in better forecast model values. More information on hydrologic data assimilation techniques can be found in (Matgen, et al., (2010); Chen, et al., 2013); García-Pintado, et al., 2015).

2.   Satellite Altimetry data applications

Satellite altimetry (figure 3) works on the principle of return echo of pulses sent from the satellite nadir point and reflected from the surfaces of open water.

The height of the water surface is extracted from the distance between the satellite and the water body with reference to a local datum given as:

$$h = R - \left(c\frac{\Delta t}{2} \right) - \Sigma cor \qquad (1)$$

where h= water level, R = distance between the satellite altimeter and the water body, c= speed of light, $\Delta t/2$ = two way travel time of radar pulse, $\sum cor$ = sum of corrections for ionospheric, wet and dry tropospheric, and tidal corrections.

This principle (figure 3) has its limitations as the accuracy of the data is affected by atmospheric conditions, sensor and satellite characteristics, and reflectance conditions (Belaud, et al., 2010).

Although satellite altimetry was developed and optimized to measure ocean level changes (not rivers), it has been demonstrated as a source of data over large rivers and lakes (Tarpanelli, et al., 2013; Jarihani, et al., 2013). Typical altimeter footprints are in kilometres; e.g. ENVISAT ranges from 1.6-10.8km, TOPEX/POSEIDON from 2.0-16.4km. Thus satellite altimetry data is used as the primary source of water level data in ungauged basins, and as a secondary data source to compare with measured data in sparsely gauged basins.

Often times the selection of altimeter water level data to be used depends on the time and season of acquisition (Papa, et al., 2012). Data acquired during high flows give better measurements than low flow season data which usually have artefacts (in the form of islets, river banks, vegetation, etc) that reduce the accuracy of the data in comparison with local gauge data. Analysing data over the Ganga-Brahmaputra Rivers, Papa, et al., (2012) got mean errors less than cm when high flow altimetry data were compared with measured data, but low flow data showed errors larger than 30cm. Siddique-E-Akbor, et al., (2011) used data from ENVISAT to compare with 1D HECRAS model output water levels in order to check for accuracy and ability to get the seasonal trend. The model was run for periods of available ENVISAT data and the output compared with the ENVISAT time series. The results showed RMSE ranging from 0.70-2.4m with the best correlation obtained during high flow seasons. The study suggest the use of calibrated hydrodynamic/ hydrologic model outputs to benchmark altimetry data in ungauged and poorly gauged catchments.

Virtual altimeter gauging stations are located at the intersection of satellite tracts with water bodies. Santos da Silver et al., (2007) used virtual altimeter stations as water level data sources for ungauged catchments. They chose the median values of virtual stations that fell within river water bodies as water levels for the river and compared with measured values from gauging stations located within 20km of the virtual stations using weighted linear regression. In order to avoid comparing two areas with different hydrological conditions, a ratio χ was computed of the discrepancy between the ENVISAT master points and the linear regression and the uncertainties associated to the ENVISAT master points. The developed method enabled a comparison that produced regression coefficient greater than 0.95 between the ENVISAT and gauges series. Santos da Silver, et al., (2012) used 533 ENVISAT virtual stations and 106 gauging data to map extreme stage variations along 32 Amazon basin rivers and analysed for drought in the catchment. Using 2005 drought and 2009 flooding events as basis, data from 2002-2005 were analysed and time series of ENVISAT per virtual station were averaged to get monthly values. Values of the mean amplitude stage variation for the measured

gauges showed good consistency with those of satellite altimetry and results for drought showed a range between -4 and 1m of anomalies. Getirana, et al., (2009) went even further and developed a rating curve of discharge values using virtual stations from ENVISAT for the upper part of the Branco River basin, Brazil. Virtual stations data were compared with nearby gauge data to check for seasonal similarity and trend, and those virtual stations with standard deviations <0.1m were chosen. The method used a distributed hydrological model to derive discharge values for the virtual stations. Model calibration and validation results showed good correlation with measured data, and the rating curve showed a 2.5-5% increase in bias when compared with rating curves from measured data. The calibration results were affected by rainfall data spatial distribution.

Although use of satellite altimetry for river stage monitoring is usually applied to large rivers with a few kilometres width (Papa, et al., 2012), altimetry data was used to estimate discharge in an ungauged part of the Po river basin (width:200-300m) using cross section data (Tarpanelli, et al., 2013). They used a simplified routing model (RCM) based on upstream data, wave travel time and hydraulic conditions on two river sections to get the flow in the second river section. The results showed good agreement between simulated and insitu discharges, and gave lower RMSEs (relative to the mean observed discharge) than calculated results using an empirical equation also based on cross section geometry. Seyler, et al., (2009) used altimetry virtual stations to estimate river slope. The calculated river slopes were used to get the river bank full discharge, and the results compared well with gauge data. Lake water volumes were calculated for Lake Mead (USA) and Lake Tana (Ethiopia) using five altimetry data products: T/P (Topex/Poseidon), Jason-1, Jason-2, GFO (Geosat Fellow On), ICESat and ENVISAT (Duan & Bastiaanssen, 2013). The method used Landsat TM/ETM + imagery data to map the water surface areas using the Modified Normalized Difference Water Index (MNDWI) method which enables robust extraction of water bodies from optical data (Zhang, et al., 2006). The calculated water surface areas agreed with in-situ measured data with an R^2 of 0.99for Lake Mead and 0.89 for Lake Tana with RMSEs of 2.19% for Lake Mead and 4.64%. The water volume was estimated using the lowest altimeter water level as the reference water level; this is then subtracted from all the other measurements to obtain the Water Level above Lowest Level (WLALL) to be used for volume estimation. Using regression analysis a relationship was established between the estimated water surface areas and the WLALL as A = f(WLALL) = aWLALL2 + bWLALL + c; where a, b, and c, are constants. The integral of this relation provides the Water Volume Above the Lowest water Level (WVALL). The estimated water volumes agreed well with in-situ water volumes for both LakeMead and Lake Tana with R2>0.95and RMSE ranging between 4.6 and 13.1%.

3. Optical satellite data

Depending on its contents, water reflects electromagnetic waves differently; pure clear water reflects differently from muddy water or water containing vegetation (floating or submerged). The amount of energy measured from the satellite sensor also depends on the bands used; blue band penetrates water up to 10m, red band is partially absorbed, and near infra-red band is totally absorbed. These sensor properties consequently affect the image, so that an image acquired using the blue band will measure reflectance from any submerged vegetation within its reach, while red/near infra-red images will show water as dark grey/ black respectively (Meijerink, et al., 2007).

With the availability of more optical satellites with relatively low temporal resolutions globally, many scenes of archived data can be accessed and used for change detection studies and flood extent mapping in areas with little cloud cover. Penton & Overton, (2007) combined flood mask extents from LandSat ETM of four flood events with LIDAR DEM to produce water heights for the floodplain. The heights of the flood mask water points were used to interpolate a water height surface which was subtracted from the DEM to produce the inundation map. To check for water surface change, satellite microwave data from AMSR-E satellite was used to calibrate CREST hydrologic model using ratio brightness temperature measurements over water bodies and calibrated dry areas (Khan, et al., 2012). The AMSR-E detected water surface signal frequency was compared with gauge flow with a probability of exceedance <25% and showed good agreement. The output of model calibrated with AMSR-E detected water surface signal showed good agreement with observed flow frequency. Results of validation were equally good with high correlation between model results and observed flows with probability of exceedance <25%. The output of the model calibrated with AMSR-E detected water surface signal showed good agreement with observed flow frequency (Nash-Sutcliff coefficient of 0.90 and a correlation coefficient of 0.80).

Due to inaccessibility of the coastal terrain, many remote wetlands and swamps have few or no gauges, and are not covered by national gridding systems. As a result such areas are not included in topographic mapping projects; even where data is available the resolution is usually very coarse and not detailed (e.g. in Ezer & Liu, 2010). The morphology of coastal areas are affected by sediment supply, sea level change, littoral transport, storm surges, as well as hydrodynamics at the river mouths of deltaic areas (Kumar, et al., 2010). Tidal flat morphology for example, changes with the tidal cycle and this can affect navigation, coastal defence, fishing, etc. The monitoring and modelling of tidal flat morphology is thus important (Mason, et al., 2010). Apart from natural causes, coastal areas are affected by human activities like sand mining, and construction of coastal infrastructure like ports, harbours, groins and other coastal defence systems.

Satellite data are used to study coastal morphological changes that affect the ecosystem and biodiversity of coastal areas. Kumar, et al., (2010) studied the morphological changes in coastal parts Karnataka State, India using satellite and ancillary data. They calculated the rate of shoreline change over a ninety five year period (1910-2005) and used the results to predict future shoreline change rates to 2029. 25 LandSat TM imageries were used to map the tidal mudflats of Cooks Inlet Alaska by integrating with an inundation model (Ezer & Liu, 2010). The morphology of Cooks Inlet is such that, tidal floods move much faster than the ebbing period which moves very slowly; therefore areas at the far end of the mudflats take several hours before tidal waters lower. To study their morphology as a test bed for prediction of floods and its effects, mapping of these frequently flooded areas was done using the LandSat imagery to delineate water only areas, and show the range of shoreline data and water levels. The model results calculated the water depth and gave the estimated 3D topography of Cooks Inlet. Similarly, four LandSat TM imagery of the Ganges -Brahmaputra River mouth taken during low-flow and high-flow seasons were used by Islam, et al., (2002) to estimate suspended sediment concentration. The method used converted the digital numbers of the imageries to radiance values and subsequently to spectral reflectance and linearly related them to suspended sediment concentration (SSC). The SSC results showed higher distribution of suspended sediments during high discharge seasons when the turbidity zone moves further seaward reaching debts of 10m, than during low flow periods when the turbidity zone remains close to the shore. Yang & Ouchic (2012) used 2000-2009 optical and SAR satellite imagery and insitu data of the Han estuary in Korea to study bar morphology by relating it with tides and precipitation using regression analysis. The results showed areas closer to the sea correlating bar size/shape with tides, and areas closer to the river mouths correlating with precipitation.

Optical satellite images of Sumatra Island were used to study post tsunami coastal recovery based on beach nourishment and sediment refilling. Liew, et al., (2010) used 1m Ikonos images of pre-tsunami, tsunami, and post tsunami periods to show that coasts affected by tsunamis naturally rebuild to their former morphological states in areas with little anthropogenic activity. The results showed straight beaches rebuilding few weeks after the tsunami, but recovery of barrier beaches and lagoons is much slower, enabling inland rivers and streams to directly discharge into the ocean. Thus, they concluded that due to the fast recovery of coastal features post tsunami, sedimentary deposits are better indicators of coastal geomorphology than tsunami events.

4.   Satellite derived DEM data applications

Satellite data provide topographic information in the form of digital elevation models (DEM's) generated from radar echoes of spot heights e.g. ASTER DEM, SRTM, and SPOT DEM. The most common and freely available DEM is the Shuttle Radar Topographic Mission (SRTM) DEM flown in February 2000 which covered 85% of the earth's surface. SRTM which was obtained through SAR interferometry of C-band signals is available in 30m and 90m spatial resolutions and an approximate vertical accuracy of 3.7m (Syvitski, et al., 2012). The vertical accuracy of SRTM is higher in areas with gentle slopes than on steep slopes; on low-lying floodplains SRTM has shown less than 2m accuracy. More information on SRTM DEM accuracy can be found in (Yan, et al., 2015; Jarihani, et al., 2015).

At the land-water boundary in areas with gentle slopes, satellite DEMs can be used to measure river stage when combined with high resolution imagery. Such combinations have been used in flood inundation mapping, although there is less accuracy in situations where the water edge is obscured by vegetation (Smith, 1997). Syvitski, et al., (2012) adjusted SRTM data using ocean heights measured by the TOPEX/POSEIDON satellite altimeter to enable the mapping of floodplain zones. Advanced microwave Scanning Radiometer (AMSR-E) data provided brightness temperature measurements of the floodplain. The ratio of land area brightness temperatures to water area brightness temperature gave the discharge estimator; chosen dry areas were used as calibration areas for measurements over water covered areas. A rating curve of the ratio versus discharge was then used to extract the discharge values. Four floodplain zones were classified around the world from the 33 floodplains studied, namely: container valleys, floodplain depressions, nodal avulsions and delta plains. SRTM data measure surface level which over river channels is equivalent to water levels when the land water boundary is delineated. Jung, et al., (2010) used insitu (bathymetry and cross sectional) data and SRTM DEM water levels to derive water surface slope, and calculate the discharge of the Brahmaputra River. The cross sectional water level was obtained by fitting a first degree polynomial function to the SRTM data elevation. The average calculated discharge results when compared to insitu gauge reading gave a difference of 2.3%. Two DEM's of the Morecambe bay were used to determine the relative change in inter-tidal sediment volume above and below mean sea level (Mason, et al., 2010). The first set of DEMs was derived from satellite SAR imagery and the second set from LiDAR. By using the sea height as zero level the LiDAR DEM was normalized to the same height as the SAR DEM. The relative change in sediment volume was derived by subtracting the normalized LiDAR DEM heights from the SAR DEM. SRTM 30m data was combined with MODIS 500m water mask data to produce 30m static water masks of 2003 flooding

along the Mississipi river (Li, et al., 2013). The method involved using SRTM to mark the minimum water level from the MODIS water mask, which is then used to calculate the maximum water-level for that pixel using a water fraction relation. All SRTM 30m pixels with heights between minimum and maximum water levels are classified as water, and all those with heights higher than the maximum level are classified as dry. Consequently, the 500m MODIS water mask is integrated into a 30m water mask with the SRTM. The results gave detailed flood maps with the same flooding coverage as the MODIS water masks but enlarged 18 times. The flood maps were compared with Landsat TM images of the flood and showed over 94% match in water area coverage. Errors/ mismatch were found to be mostly around areas with trees and vegetation cover.

3. Future needs and direction

1.   Gaps and limitations

As useful as satellite data applications have been in estimating surface water parameters, the measurements come with limitations due to sensor specifications/ errors, pre and post data processing techniques, calibration, measurement conditions, satellite distance from the targets, etc. Optical satellite data for example is limited to day time acquisition due to its dependence on sunlight, and is not very useful in areas perpetually covered by clouds because the target cannot be reached (Smith, 1997).

Since satellite data is used for calibration, its accuracy when compared with measured data is very important. Satellite data accuracy is estimated using different error measurement techniques (e.g. RMSE, Mean error), checking for correlation with measured data, or measuring the coefficient of determination (e.g. Tarpanelli, et al., 2013). There are multiple sources of error that can affect the data; for example the uncertainties in using satellite river width for calibration include: the satellite estimation of the river width, the power relation between the discharge and river width (which is an approximation of the conditions at a river cross section when there is no backwater effect) and the assumption of a stable/static river cross section. However these sources of uncertainty are lowest for the period of satellite data acquisition and increase in with change in season and hydraulic conditions (Sun, et al., 2010).

SAR

The quality and usefulness of SAR data for hydrological studies depends on meteorological conditions (wind and rain), emergent vegetation, incidence angle and the polarisation mode used for

data acquisition. Horizontal - Horizontal (HH) polarisation gives better results for flood extent mapping than Vertical - Horizontal (VH) and Vertical - Vertical (VV) polarisations. However, VH and VV polarisations are also useful since VV polarisation data highlight vertical features like vegetation, and VH polarisation data reflect the horizontal nature of the smoothed flood water (Schumann, et al., 2007). Another important factor for SAR data use in hydrology is the river size. Until the recent launch of CSK, RADARSAT-2, PALSAR, and TerraSAR-X, most available SAR satellites had large spatial resolutions which excluded smaller rivers from being captured; since it was difficult to delineate them in an image (Sun, et al., 2009).

Satellite SAR used for delineation of water extent has the limitation of floodplain vegetation being included and classified as water pixels; more so the height of the SAR waterline does not show the variation in water height with flow direction.

Altimetry

For river stage estimation and wetlands delineation, problems encountered with satellite altimetry data include: incorrect processing of radar echoes over rivers/lakes by satellite trackers, poor temporal resolution, and lack of information within the data about the atmospheric wet vapour content over lakes/rivers (Crétaux, et al., 2009). The errors recorded while using altimeter water level data can however be increased by incorrect choice of data; which frequently occurs when dry area data is retained within the data for computing water stages in low flow seasons (Santos da Silva, et al., 2007). The difference between altimeter and gauge measurements also increases with distance between the points, topography and river width (León, et al., 2006). When compared with gauge data, RMSEs of altimetry data measured over the Amazon have ranges from 30cm-70cm using data from ENVISAT, ERS2, and GeoSaT (Tarpanelli, et al., 2013),however at cross track situations where altimetry measurements are taken at the same location with a gauging station the difference can be <20cm (Seyler, et al., 2009). The accuracy of altimeter measurements over rivers is also affected by the river width and the morphology of the river banks so that data on narrow rivers and vegetated banks have lower accuracy (Papa, et al., 2012). Furthermore, the specifications of the altimetry system itself can affect quality of measurements; for example ENVISAT data have been shown to have lower RMSE compared to ERS2 data due to ENVISATs ability to switch frequency modes in response to change in terrain and its smaller bin width (Tarpanelli, et al., 2013).

DEM

The limitation of satellite DEM is in the data quality. DEM data needed for modelling and other analyses that require topographic data depends on the acquisition method, the data processing and the characteristics of the mapped terrain. Satellite derived DEMs have less vertical accuracy, higher bias and higher RMSE than other DEMS derived from airborne LIDAR and airborne IFSAR (Fraser & Ravanbakhsh, 2011).

In spite of their limited accuracy satellite DEMs have global or almost global coverage unlike airborne DEMs. Therefore they are useful sources of topographic data especially for low lying coastal areas with gentle slopes (Gorokhovich & Voustianiouk, 2006; Schumann, et al., 2008); and consequently applicable for inundation modelling (Karlsson & Arnberg, 2011). Figure 4 shows results of flood modelling undertaken for the Lower Niger River (Nigeria) using SRTM 30 and 90m. The Niger River overflowed its banks in 2007 and flooded a large part of the floodplain. MODIS satellite data was used to map the flood and provided the only reference record of the flood. Figure 4 shows that the model results are comparable with the MODIS flooding extent.

Generally satellite based DEMs are either generated from radar echoes of spot heights, or from SAR interferometry. However Mason et al., (2010) also derived DEMs from SAR images. The method involved using SAR water height to interpolate a set of waterlines, which were then used to produce a 50m DEM of the intertidal zone with an accuracy of 40cm. The method is however limited by the temporal de-correlation of the waterline heights.

2.   Current data use strategies

Innovative methodologies are being introduced by scientists to better exploit satellite data to overcome the data limitations within present uncertainties. For example cloud filtering techniques have been developed that remove a high percentage of the clouds in optical data, thus adding to data availability. In terms of temporal limitations, combining MODIS data with its high temporal resolution with other types of satellite data is a technique that is now exploited more (Jarihani, et al., 2014). The technique generates new datasets that blend higher spatial resolution at the high temporal resolution of MODIS. When combined with DEM data for example, flood maps that provide daily information can be easily generated (Li, et al., 2013). SRTM has been combined with MODIS data to generate a 250m water mask called MOD44W; because of the high temporal resolution of MODIS this product can be updated regularly to provide static water masks (Li, et al., 2013).

Use of Satellite SAR for flood extent mapping and model calibration can be improved through combination with other higher resolution data to increase precision in flood height determination. To improve the vertical accuracy of SAR waterline extent during floods, Mason, et al., (2007) used waterline data extracted from ERS-1 SAR corrected with 1m resolution LIDAR heights (along the Thames River bank) to calibrate a LISFLOOD model of flood extent. The output waterline when compared with waterline measured from aerial photos showed a lower root mean squared error than those obtained using SAR data only.

Satellite DEMs that are enhanced through vegetation smoothing or hydrological correction have shown lower errors compared with the original data (Jarihani et al., 2015). Due to the availability of the hydrologically corrected SRTM DEM, a global static 30-m water mask has been generated which is very useful for flood detection especially in data scarce areas.

To improve the use of satellite altimetry data, interpolation methods have been developed to correct the data accuracy and precision by comparing the data with lakes and reservoir measurements. Thus the correlation with measured gauge data, range of RMSE and reduction in discrepancies have improved to levels >0.95 correlation during validation (Ričko, et al., 2012). Altimeter measurements over modified channels is however less reliable than that of natural catchments (Kim, et al., 2009).

The use of altimeter data is also limited by the poor temporal resolution of satellite altimeters; which range from days to several weeks. Belaud, et al., (2010) developed a method to interpolate river water levels in-between satellite observations in order to provide continuous data. The developed method used upstream ground station measurements and altimetry data as output to calibrate a propagation model by adjusting the satellite observed values. The propagation model used a transfer function to predict water level variations based on the relationship between the propagation times and water levels. The results were able to predict flood peaks during periods of no satellite coverage. Crétaux, et al., (2011) addressed the problem of data gaps by combining three sets of altimetry data (TOPEX/POSEIDON, ENVISAT1 and JASON2) with MODIS measurements of water extent to monitor wetlands and floodplains in arid/semi arid regions. The MODIS data was used to classify the open water pixels whose relative values were then extracted from altimetry data. The results provided relative water heights, due to the low temporal resolution of the altimetry data sets. Altimeter data from ICESat was used to calibrate a large scale LISFLOOD-FP hydro-dynamic flood model of the Zambezi River, Mozambique (Schumann, et al., 2013). Eight in-channel water levels from ICESat from one altimeter pass were used for calibration of model output. The models with a mean bias within one standard deviation of the ICESat values were accepted as comparable with Landsat measured flooding extents. The results showed 86% agreement between the Landsat flood

extent and the accepted model outputs; corresponding to mean distance of 1.42-1.60 km. After calibration the model upstream boundary was changed to forecast flow values in order to forecast downstream flooding. The results correlated with the baseline model, but showed that with a lead time of 5 days, better basin wide precipitation observations will enable flood forecasting on the Zambezi.

3.   Future direction

Available literature show that efforts have been made to develop an empirical relationship between satellites derived surface water extents (including flooded areas) with river stage or discharge. Such a relationship has been established for braided rivers; for non-braided rivers the results have depended on the river system, thus inundation area can increase or decrease with stage. With better SAR missions such as TerraSAR-X- TanDEM-X formation, DEM data with good vertical accuracy are now available for better hydraulic flood modelling. TanDEM-X has 12.5m spatial resolution and produces less than 2m vertical accuracy (DLR, 2015). Although made for polar ice change estimation and monitoring, the high spatial coverage of Cryosat-2 is also being exploited for near-shore mapping and inland water monitoring (Villladsen, Andersen, & Stenseng, 2014). Cryosat-2 which operates in SAR and interferometric modes, has a drifting orbit and therefore (unlike all the other satellites) has little repetitive data (since repeat cycle is 369 days). Its high spatial density coverage makes it good for hydraulic modelling (and all its evaluations have produced good results). With successful use of Cryosat-2 data to obtain river water levels and topography, the use of drifting orbits is being proposed as more suitable for river water surface topography mapping, derivation of river profiles and building of pseudo time series (Bercher, et al., 2014).

Other satellite products that improve the accuracy of satellite data based research in hydrology include: Cosmo-SkyMed from the Italian Space Agency, RadarSat2 from the Canadian Space Agency, and Sentinel-1 from ESA (Schumann, et al., 2015). Others are Global Change Observation mission-water (GCOM-W) from Japan Space Agency (JAXA), Global Precipitation Measurement (GPM) from JAXA /USA, Soil Moisture Active Passive (SMAP) from USA.

To improve quality of satellite SAR and topographic data, new satellite missions with higher precision instruments are being planned. One of such missions is the Sentinel constellation that will consist of seven satellites; two of which (Sentinel 3 and 6) are especially dedicated to hydrological purposes. Sentinel 1 is already in orbit and undergoing calibration; it has a C-band SAR instrument to continue present C-band data provision. Sentinel 3 is planned to provide fast data for flood emergencies, therefore it has three instruments one of which is a dual-frequency (Ku and C band)

advanced Synthetic Aperture Radar Altimeter (SRAL) that will provide accurate topographic data of oceans, ice sheets, sea ice, rivers and lakes (ESA, 2015). Sentinel 6, which will compliment the Sentinel 3 data, will carry on board a high precision radar altimeter. RADARSAT constellation, a new Low Earth Orbit (LEO) C-band SAR mission is under development by the Canadian space Agency (CSA). The constellation which will have several operating modes will provide interferometric SAR data that can be used for wetlands and coastal change mapping, flood disaster warning and response with resolutions 3, 5, 16, 30, 50 and 100m (Canadian Space Agency (CSA), 2015).

Other upcoming satellite missions like Surface Water & Ocean Topography (SWOT) made especially to survey global surface water have specifications that will enable better use of satellite data in hydrology. SWOT which uses a wide-swath altimetry technology will also observe the fine details of the ocean's surface topography, and measure how water bodies change over time with repeated high-resolution elevation measurements. The mission, scheduled to be launched in 2020 is an international collaboration between the US National Aeronautics and Space Agency (NASA) and Centre National E'tudes Spatiales (CNES) of France; supported by the Canadian Space Agency (CSA) and the UK Space Agency (UKSA) (Pavelsky, et al., 2015). Another product of international cooperation that will support hydrological research is the Jason3 altimetry mission from NOAA, due to be launched in July 2015. The Jason3 mission is dedicated to the measurement of sea surface height, wave, wind speed, and will provide useful data to monitor sea level rise, coastal areas modelling of oil spills, forecasting of hurricanes etc. To enable precise detection of sea level change, Jason3 combines GPS, radar altimetry, and a microwave radiometer to produce data within 1cm accuracy every 10 days (NOAA, 2015). Jason3 is jointly owned by US National Oceanic and Atmospheric Adminitration (NOAA), CNES-France, European Organisation for the Exploitation of Meteorological Satellites (EUMETSAT), and US NASA.

4. Conclusions

Satellite remote sensing provides a source of hydrological data that is unhindered by geopolitical boundaries, has access to remote/unreachable areas, and provides frequent and reliable data (Jung, et al., 2010). Use of satellite data to estimate hydrological parameters continues to increase due to greater availability of satellite data, improvement in knowledge of and utilization of satellite data, as well as expansion of research topics. A very important catalyst to this growth in satellite data utilization is the ability to use it in a GIS environment. GIS enables comparison and deduction of

relationships that exist amongst the complex data sources used for analysis. Thus relationships like the effects of land-use change on surrounding water bodies or water management are easily analysed and depicted. Consequently, satellite data is commonly used for: mapping of water bodies, testing of inundation models, soil moisture measurements, precipitation monitoring, estimation of evapotranspiration, and mapping of flood extent.

Data quality, pre/post data processing etc, introduce new errors and increase the uncertainties in satellite data utilization. However several methods have been developed to quantify the errors and produce acceptable results. Moreover, a number of satellite missions to address issues of climate change are being planned; some of these are dedicated to water resources management and will carry high precision instruments. The products of these missions will have less error; consequently results obtained will more accurate, thereby filling the gap in data availability.

Author contributions

The authors worked together as a team in developing the review paper.

Acknowledgements

References

Anderson, R. G., Lo, M.-H., & Famigliett, J. S. (2012). Assessing surface water consumption using remotely-sensed groundwater, evapotranspiration, and precipitation. *Geophysical Research Letters, 39*, L16401. doi:10.1029/2012GL052400

Barneveld, H., Silander, J., Sane, M., & Malnes, E. (2008). Application of satellite data for improved flood forecasting and mapping. 4th International Symposium on Flood Defence:Managing Flood Risk, Reliability and Vulnerability May 6-8, 2008 Toronto, Canada. Retrieved from http://www.hkv.nl/site/hkv/upload/publication/Application_of_satellite_data_for_improved_flood_fo recasting_HJB.pdf (Last access: 01-June 2015)

Bastiaanssen, W., Menenti, M., Feddes, R. A., & Holtslag, A. (1998). A remote sensing surface energy balance algorithm for land (SEBAL)1. Formulation. *Journal of Hydrology, 212-213*, 198–212.

Belaud, G., Cassan, L., & Bader, J. C. (2010). Calibration of a propagation model in large river using satellite. Edited by A. I. Stamou (Hrsg.), *6th International Symposium on Environmental Hydraulics* (S. 869–874). Athens, Greece: CRC PRESS. Environmental Hydraulics.

Bercher, N., Calmant, S., Picot, N., Seyler, F., & Fleury, S. (2014). *Evaluation of Cryosat-2 measurements for the monitoring of large river water levels.* Retrieved from: Along-Track.com: http://chronos.altihydrolab.fr/2012-09-23%20Venice%20ESA%2020%20years%20of%20progress%20in%20altimetry/Bercher.2012b%20(Venice%20Paper)%20CryoSat-2%20hydro.pdf (Last access 25-06-2015)

Canadian Space Agency (CSA). (2015). *RADARSAT Constellation.* Retrieved from RADARSAT constellation: http://www.asc-csa.gc.ca/eng/satellites/radarsat/ (Last access June 23, 2015)

Chen, H., Yang, D., Hong, Y., Gourley, J., & Zhang, Y. (2013). Hydrological data assimilation with the Ensemble Square-Root-Filter:Use of streamflow observations to update model states for real-time flash flood forecasting. *Advances in Water Resources, 59*, 209–220. doi:10.1016/j.advwatres.2013.06.010

Crétaux, J. F., Stéphane, C., Romanovski, V., Shabunin, A., Lyard, F., Bergé Nguyen, M., . . . Perosanz, F. (2009). An absolute calibration site for radar altimeters in the continental domain : lake Issykkul in Central Asia. *Journal of Geodesy, 83*(8), 723-735.

Crétaux, J., Bergé-Nguyen, M., Leblanc, M., Del Rio, R. A., Delclaux, F., Mognard, N., . . . Maisongrande, P. (2011). Flood mapping inferred from remote sensing data. *Fifteenth International Water Technology Conference.* Alexandria, Egypt, 28-30 May, 2011.

Dellepiane, S., de Laurentiis, R., & Giordano, F. (2004). Coastline Extraction from SAR Images and a Method for the Evaluation of the Coastline Precision. *Pattern Recognition Letters, 25*, 1461–1470.

Di Baldassarre, G., Schumann, G., & Bates, P. D. (2009). A technique for the calibration of hydraulic models using uncertain satellite observations of flood extent. *Journal of Hydrology, 367*(3-4), 276–282. doi:10.1016/j.jhydrol.2009.01.020

DLR. (2015). *Earth Observation: TanDEM-X - the Earth in three dimensions*. Retrieved from http://www.dlr.de/dlr/en/desktopdefault.aspx/tabid-10378/566_read-426/#/gallery/345 (Last access: 01-June-2015)

Duan, Z., & Bastiaanssen, W. (2013). Estimating water volume variations in lakes and reservoirs from four operational satellite altimetry databases and satellite imagery data. *Remote Sensing of Environment, 134*, 403–416. doi:10.1016/j.rse.2013.03.010

ESA. (2015). *Sentinel 3*. Retrieved from Copernicus, observing the Earth: http://www.esa.int/Our_Activities/Observing_the_Earth/Copernicus/Sentinel-3 (Last access June 15, 2015)

Ezer, T., & Liu, H. (2010). On the dynamics and morphology of extensive tidal mudflats: Integrating remote sensing data with an inundation model of Cook Inlet, Alaska. *Ocean Dynamics, 60*(5), 1307-1318. doi:10.1007/s10236-010-0319-x

Fraser, C. S., & Ravanbakhsh, M. (2011). PERFORMANCE OF DEM GENERATION TECHNOLOGIES IN COASTAL ENVIRONMENTS. *7th International Symposium on Digital Earth.* 40-49, Perth, Australia, 23-25 August 2011.

García-Pintado, J., Mason, D., Dance, S., Cloke, H., Neal, J., Freer, J., & Bates, P. (2015). Satellite-supported flood forecasting in river networks: A real case study. *Journal of Hydrology, 523*, 706–724. doi:10.1016/j.jhydrol.2015.01.084

Getirana, A. C., Bonnet, M.-P., Calmant, S., Roux, E., Rotunno Filho, O. C., & Mansur, W. J. (2009). Hydrological monitoring of poorly gauged basins based on rainfall–runoff. *Journal of Hydrology, 379*, 205–219. doi:0.1016/j.jhydrol.2009.09.049

Giustarini, L., Matgen, P., Hostache, R., Montanari, M., Plaza, D., Pauwels, V., . . . Savenije, H. (2011). Assimilating SAR-derived water level data into a hydraulic model:a case study. *Hydrology and Earth System Sciences, 15*, 2349–2365. doi:10.5194/hess-15-2349-2011

Gorokhovich, Y., & Voustianiouk, A. (2006). Accuracy assessment of the processed SRTM-based elevation data by CGIAR using field data from USA and Thailand and its relation to the terrain characteristics. *Remote Sensing of Environment, 104*, 409–415. doi:10.1016/j.rse.2006.05.012

Horritt, M. S. (2006). A methodology for the validation of uncertain flood inundation models. *Journal of Hydrology, 326*(1-4), 153–165. doi:10.1016/j.jhydrol.2005.10.027

Islam, R. Z., Begum, S. F., Yamaguchi, Y., & Ogawa, K. (2002). Distribution of suspended sediment in the coastal sea off the Ganges–Brahmaputra River mouth: observation from TM data. *Marine Systems, 32*(4), 307–321. doi:10.1016/S0924-7963(02)00045-3

Jarihani, A., Callow, J., Johansen, K., & Gouweleeuw, B. (2013). Evaluation of multiple satellite altimetry data for studying inland water bodies and river floods. *Journal of Hydrology, 505*, 78–90. doi:10.1016/j.jhydrol.2013.09.010

Jarihani, A., Callow, J., McVicar, T., Van Niel, T., & Larsen, J. (2015). Satellite-derived Digital Elevation Model (DEM) selection, preparation and correction for hydrodynamic modelling in large, low-gradient and data-sparse catchments. *Journal of Hydrology, 524*, 489–506. doi:10.1016/j.jhydrol.2015.02.049

Jarihani, A., McVicar, T., Van Niel, T., Emelyanova, I., Callow, J., & Johansen, K. (2014). Blending Landsat and MODIS Data to Generate Multispectral Indices: A Comparison of "Index-then-Blend" and "Blend-then-Index" Approaches. *Remote Sensing, 6*, 9213-9238. doi:10.3390/rs6109213

Jung, C. H., Hamski, J., Durand, M., Alsdorf, D., Hossain, F., Lee, H., and Hasan, K. (2010). Characterization of complex fluvial systems using remote sensing of spatial and temporal water level variations in the Amazon, Congo, and Brahmaputra Rivers. *Earth Surface Processes and Landforms, 35*(3), 294-304. doi:10.1002/esp.1914

KARLSSON, J. M., & ARNBERG, W. (2011). Quality analysis of SRTM and HYDRO1K: a case study of flood inundation in Mozambique. *International Journal of Remote Sensing, 32*(1), 267-285. doi:10.1080/01431160903464112

Khan, S. I., Hong, Y., Vergara, H. J., Gourley, J. J., Brakenridge, G. R., De Groeve, T., and Yong, B. (2012). Microwave Satllite Data for Hydrologic Modelling in Ungauged Basins. *IEEE Geoscience and Remote Sensing Letters, 9*(4). doi:0.1109/LGRS.2011.2177807

Kim, J., Lu, Z., Lee, H., Shum, C. K., Swarzenski, C. M., Doyle, T. W., & Baek, S.-H. (2009). Integrated analysis of PALSAR/Radarsat-1 InSAR and ENVISAT altimeter data for mapping of absolute water level changes in Louisiana wetlands. *Remote Sensing of Environment, 113*(11), 2356-2365.

Kumar, A., Narayana, A., & Jayappa, K. (2010). Shoreline changes and morphology of spits along southern Karnataka, west coast of India: A remote sensing and statistics-based approach. *Geomorphology, 120*, 133–152. doi:10.1016/j.geomorph.2010.02.023

León, J. G., Calmant, S., Seyler, F., Bonnet, M.-P., Cauhopé, M., Frappart, F., and. Fraizy, P. (2006). Rating curves and estimation of average water depth at the upper Negro. *Journal of Hydrology, 328*, 481-496. doi: 10.1016/J.JHYDROL.2005.12.006

Li, S., Sun, D., Goldberg, M., & Stefanidis, A. (2013). Derivation of 30-m-resolution water maps from TERRA/MODIS and SRTM. *Remote Sensing of Environment, 134*, 417–430. doi:10.1016/j.rse.2013.03.015

Liew, S. C., Gupta, A., Wong, P. P., & Kwoha, L. K. (2010). Recovery from a large tsunami mapped over time: The Aceh coast, Sumatra. *Geology, 114*(4), 520-529. doi:10.1016/j.geomorph.2009.08.010

Lillesand, T., Kiefer, R. W., & Chapman, J. W. (2004). *Remote sensing and image interpretation.* (5th, Hrsg.) John Wiley and sons, Hobone, NJ USA.

Long, S., Fatoyinbo, T., & Policelli, F. (2014). Flood extent mapping for Namibia using change detection and thresholding with SAR. *Environmental Research Letters, 9*(035002). doi:10.1088/1748-9326/9/3/035002

Mason, D. C., Horritt, M. S., Dall'Amico, J. T., & Scott, T. R. (2007). Improving River Flood Extent Delineation From Synthetic Aperture Radar Using Airborne Laser Altimetry. *IEEE Transactions on Geoscience and Remote Sensing and*(0196-2892), 3932 - 3943. doi:10.1109/TGRS.2007.901032

Mason, D. C., Scott, T. R., & Dance, S. L. (2010). Remote sensing of intertidal morphological change in Morcambe Bay, U,K., between 1991 and 2007. *Estuarine , Coastal and Shelf Science, 87*, 487-496. doi:10.1016/j.ecss.2010.01.015

Matgen, P., Montanari, M., Hostache, R., Pfister, L., Hoffmann, L., Plaza, D., and Savenije, H. (2010). Towards the sequential assimilation of SAR-derived water stages into hydraulic models using the Particle Filter: proof of concept. *Hydrology and Earth System Sciences, 14*, 1773–1785. doi:10.5194/hess-14-1773-2010

Mcmillan, H., Hreinsson, E., Clark, M., Singh, S., Zammit, C., & Uddstrom, M. (2013). Operational hydrological data assimilation with the recursive ensemble Kalman filter. *Hydrology and Earth System Sciences, 17*, 21-38. doi:10.5194/hess-17-21-2013

Meijerink, A. M., Bannert, D., Batelaan, O., Lubczynski, M. W., & Pointet, T. (2007). *Remote sensing applictions to groundwater.* Series on Groundwater, UNESCO, Paris,France.

NOAA, S. I. (2015). Jason3. Retrieved from http://www.nesdis.noaa.gov/jason-3/?CFID=731ecb89-8379-48fc-ad50-9546e71739&CFTOKEN=0 (Last access: May 29 2015).

Noh, S., Tachikawa, Y., Shiiba, M., & Kim, S. (2011). Applying sequential Monte Carlo methods into a distributedhydrologic model: lagged particle filtering approach with regularization. *Hydrology and Earth System Sciences, 15*, 3237–3251,. doi:10.5194/hess-15-3237-2011

Owe, M., Brubaker, K., Ritchie, J., & Albert, R. (2001). *Remote sensing and Hydrology, 2000.* IAHS, Wallingford OX, UK.

Papa, F., Bala, S. K., Pandey, R. K., Durand, F., Gopalakrishna, V. V., Rahman, A., and Rossow, W. B. (2012). Ganga-Brahmaputra river discharge from Jason-2 radar altimetry: An update to the long-term satellite-derived estimates of continental freshwater forcing flux into the Bay of Bengal. *Journal of Geophysical Research, 117*(C11021). doi:10.1029/2012JC008158

Pavelsky, T., Morrow, R., Peterson, C., Andral, A., Bronner, E., & Srinivasan, M. (2015). *SWOT 101: A Quatum Improvement of Oceanography and Hydrology from the Next Generation Altimeter Mission.* Retrieved from: Surface Water and Ocean Topography: https://swot.jpl.nasa.gov/files/swot/SWOT-101_Jan2015.pdf (Last access: 29. May 2015)

Penton, D. J., & Overton, I. C. (2007). Spatial modelling of floodplain inundation combining satellite imagery and elevation models. *MODSIM 2007 International Congress on Modelling and Simulation.* Modelling and Simulation Society of Australia and New Zealand CSIRO,CClayton south, Vic,Australia.

Pereira-Cardenal, S. J., Riegels, N. D., Berry, P. A., Smith, R. G., Yakovlev, A., Siegfried, T. U., & Bauer-Gottwein, P. (2011). Real-time remote sensing driven river basin modeling using radar altimetry. *Hydrology and Earth sciences*, 241-254. doi:10.5194/hess-15-241-2011

Quinn, P.F., Hewett, C.J.M., Muste, M., Popescu, I.(2010) Towards new types of water-centric collaboration. *Proceedings of the Institution of Civil Engineers: Water Management*, 163 (1), 39-51. DOI: 10.1680/wama.2010.163.1.39

Rička, M., Birkett, ,. C., Carton, ,. J., & Crétauxc, J.-F. (2012). Intercomparison and validation of continental water. *Journal of Applied Remote Sensing, 6*. Retrieved from Terms of Use: http://spiedl.org/terms (last access: 03/12/2013)

Sarhadi, A., Soltani, S., & Modarres, R. (2012). Probabilistic flood inundation mapping of ungauged rivers: Linking GIS techniques and frequency analysis. *Journal of Hydrology, 458-459*, 68-86. doi:10.1016/j.jhydrol.2012.06.039

Santos da Silva, J., Roux, E., Filho, O., Bonne, M. P., Seyler, F., & Calmant, S. (2007). 3D Selection of Envisat Data for Improved Water Stage Times Series on the Rio Negro and Adjacent Wetlands (Amazon Basin). *2nd Hydrospace Workshop, 07_06.* ESA.Geneva, 12-14 November.

Santos da Silver, J., Calmant, S., Seyler, F., Lee, H., & Shum, C. (2012). Mapping of the extreme stage variations using ENVISAT altimetry in the Amazon basin rivers. *International Water Technology Journal, IWTJ, 2*(1), 14-25.

Schumann, G. J.-P., Bates, P., Neal, J., & Andreadis, K. (2015). Measuring and Mapping Flood processes. In P. Paron, & G. Di Baldassare (Hrsg.), *Hydro-Meteorological Hazards, Risks, and Disasters* (S. 35-64). Amsterdam,Netherlands: Elsevier.

Schumann, G. J.-P., Neal, J., Voisin, N., Andreadis, K., Pappenberger, F., Phanthuwongpakdee, N., and Bates, P. (2013). A first large-scale flood inundation forecasting model. *Water Resources Research, 49*, 6248–6257. doi:10.1002/wrcr.20521, 2013

Schumann, G., Matgen, P., Cutler, M., Black, A., Hoffmann, L., & Pfister, L. (2008). Comparison of remotely sensed water stages from LiDAR,topographic contours and SRTM. *Photogrammetry and Remote Sensing, 63*, 283–296. doi:10.1016/j.isprsjprs.2007.09.004

Schumann, G., Matgen, P., Hoffmann, L., Hostache, R., Pappenberger, F., & Pfister, L. (2007). Deriving distributed roughness values from satellite radar data for flood inundation modelling. *Journal of Hydrology, 344*(1-2), 96–111. doi:10.1016/j.jhydrol.2007.06.024

Schumann, G., Matgen, P., Pappenberger, F., Black, A., Cutler, M., Hoffmann, L., & Pfister, L. (2006). The Refix Model: Remote Sensing Based Flood Modelling. *ISPRS Commission VII Mid-term Symposium "Remote Sensing: From Pixels to Processes.* Enschede, the Netherlands: ISPRS COMMISSION.

Seyler, F., Calmant, S., Santos da Silva, J., León, G. J., Frappart, F., Bonnet, M.-P., . . . Seyler, P. (2009). New perspectives in monitoring water resources in large tropical transboundary basins based on the combined used of remote sensing and radar altimetry. *Improving Integrated Surface and*

Groundwater Resources Management in a Vulnerable and Changing World, IAHS Publication, Wallingford OX, UK, 282-288. doi:10.13140/2.1.5101.0569

Siddique-E-Akbor, A. H., Hossain, F., Lee, H., & Shum, C. K. (2011). Inter-comparison study of water level estimates derived from. *Remote Sensing of Environment, 115*(6), 522–1531. doi:10.1016/j.rse.2011.02.011

Skakun, S. (2010). A neural network approach to flood mapping using satellite imagery. *Computing and Informatics, 29*, 1013–1024.

Smith, L. C. (1997). Satellite Remote Sensing of River Innundation Area, Stage and Discharge: A review. *Hydrological Processes, 11*, 1427-1439.

Sun, A. Y., Green, R., Swenson, S., & Rodell, M. (2012). Towards Calibration of Regional Groundwater models using GRACE data. *Journal of Hydrology, 422-423*, 1-9. doi:10.1016/j.jhydrol.2011.10.025

Sun, W., Ishidaira, H., & Bastola, S. (2009). Estimating discharge by calibrating hydrological model against water surface width measured from satellites in large ungauged basins. *Annual Journal of Hydraulic Engineering, 53*, 49-54.

Sun, W., Ishidaira, H., & Bastola, S. (2010). Towards improving river discharge estimation in ungauged basins: calibration of rainfall-runoff models based on satellite observations of river flow width at basin outlet. *Hydrology and Earth Sysytem Sciences, 14*, 2011–2022. doi:10.5194/hess-14-2011-2010

Syvitski, J. P., Overeem, I., Brakenridge, R. G., & Hannon, M. (2012). Floods, floodplains, delta plains — A satellite imaging approach. *Sedimentary Geology, 267-268*, 1-14. doi:10.1016/j.sedgeo.2012.05.014

Tarpanelli, A., Barbetta, S., Brocca, L., & Moramarco, T. (2013). River Discharge Estimation by Using Altimetry Data and Simplified Flood Routing Modeling. *Remote Sensing, 5*, 4145-4162. doi:10.3390/rs5094145

Vermeulen, C. J., Barneveld, H. J., Huizinga, H. J., & Havinga, F. J. (2005). Data-assimilation in flood forecasting using time series and satellite data. *International conference on innovation advances and implementation of flood forcasting technology.* Tromso: ACTIF/Floodman/FloodRelief.

Villladsen, H., Andersen, O., & Stenseng, L. (2014). Annual cycle in lakes and rivers from cryosat-2 altimetry - the brahmaputra river. *International Geoscience and Remote Sensing Symposium (IGARSS)* (pp. 894-897). 13-18 July 2014. Quebec, Canada: IEEE. doi:978-1-4799-5775-0/14

Westahoff, R., Huizinga, J., Kleuskens, M., Burren, R., & Casey, S. (2010). ESA Living Planet Symposium. *686.* Bergen, Norway: ESA Communications.

Woldemicheal, A., Degu, A., Siddique-E-Akbor, A., & Hossain, F. (2010). Role of Land–Water Classification and Manning's Roughness Parameter in Space-Borne Estimation of Discharge for Braided Rivers: A Case Study of the Brahmaputra River in Bangladesh. *IEEE Journal of Selected Topics in Applied Earth Observations and Remote Sensing*. doi:10.1109/JSTARS.2010.2050579

Yan, K., Di Baldassarre, G., Solomatine, D., & Schumann, G. (2015). A review of low-cost space-borne data for flood modelling:topography, flood extent and water level. *Hydrological processes*. doi:10.1002/hyp.10449

Yang, C., & Ouchic, K. (2012). Analysis of bar morphology using multi-temporal and multi-sensor satellite images: Example from the Han Estuary, Korea. *Marine Geology, 311-314*, 17–31. doi:10.1016/j.margeo.2012.04.004

Zhang, J., Xu, K., Yang, Y., Qi, L., Hayashi, S., & Watanabe, M. (2006). Measuring water storage fluctuations in Lake Dongting, China, by Topex/Poseidon satellite altimetry. *Environmental Monitoring and Assessment, 115*, 23-37. doi:10.1007/s10661-006-5233-9

Table 1. Some satellite mission and sensors used for hydrological studies.

Mission	Sensor (s)	Application (hydrological)
Aqua	AIRS, AMSR-E, AMSU-A, CERES, HiRDLS, HSB, MODIS	Surface temperatures of land and ocean. (Flood mapping)
CryoSat	DORIS-NG, Laser Reflectors (ESA), SIRAL	Ice thickness (Applied also for near-shore mapping and inland water monitoring)
Envisat	AATSR, ASAR, ASAR	Physical oceanography, ice

|		
	(image mode), ASAR (wave mode), DORIS-NG, MERIS, MIPAS	and snow, (Ocean/ river water level altimetry)
ERS 1	AMI/SAR/Image, AMI/SAR/Wave,	Earth Resources, Physical oceanography (altimetry)
ERS 2	AMI/Scatterometer, ATSR AMI/SAR/Image,AMI/SAR/Wave, AMI/Scatterometer, ATSR/M	Earth resources, Physical oceanography (altimetry)
Jason 1	DORIS-NG, JMR, LRA, POSEIDON-2 (SSALT-2), TRSR	Physical oceanography (Ocean/River water level altimetry)
Jason 2	AMR, DORIS-NG, GPSP, JMR, LRA, POSEIDON-3	Physical oceanography (altimetry)
Radarsat 1/2	C-Band SAR, X-Band SAR	Flood mapping/modelling
Sentinel 1	C-Band SAR	Flood mapping/ modelling
SRTM	C-Band SAR, X-Band SAR	Digital elevation models, flood modelling
SPOT 4	DORIS (SPOT), HRVIR, VEGETATION	Digital terrain models, environmental monitoring
SPOT 5	DORIS-NG (SPOT), HRG, HRS, VEGETATION	Digital terrain models, environmental monitoring
Terra	MODIS, MOPITT, MISR, ASTER, CERES	Physical processes, surface temperatures of land and ocean (surface water mapping)
Topex/Poseidon	DORIS, LRA, POSEIDON-1 (SSALT-1), TMR, TOPEX	Physical oceanography (altimetry)
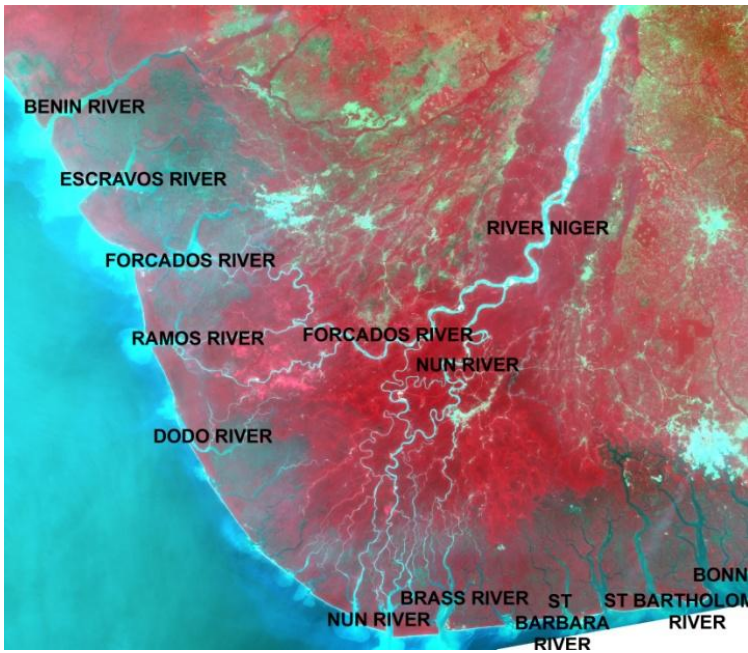
Figure 1. NigeriaSatX satellite image showing rivers in the Niger delta
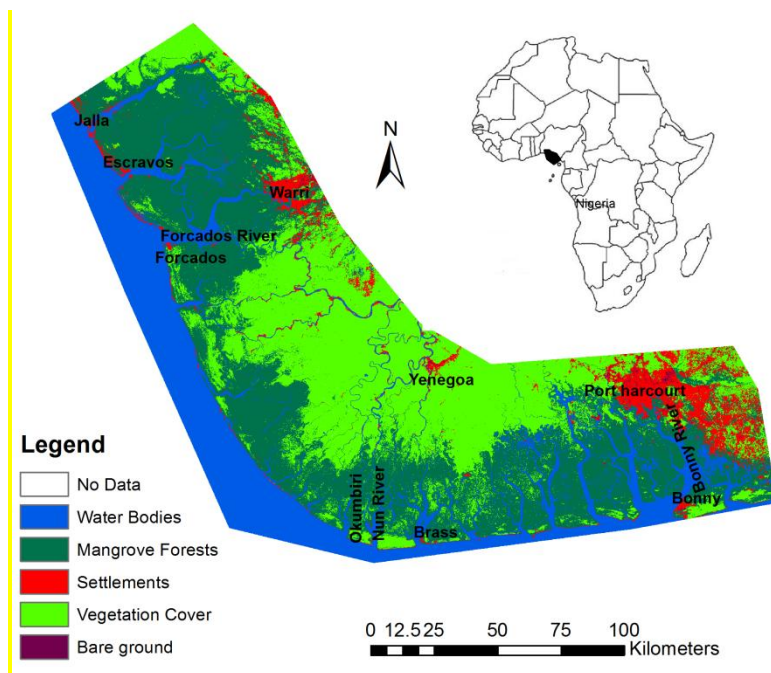

Figure 2. Classified NigeriaSat-1 image of the Niger delta showing five feature classes
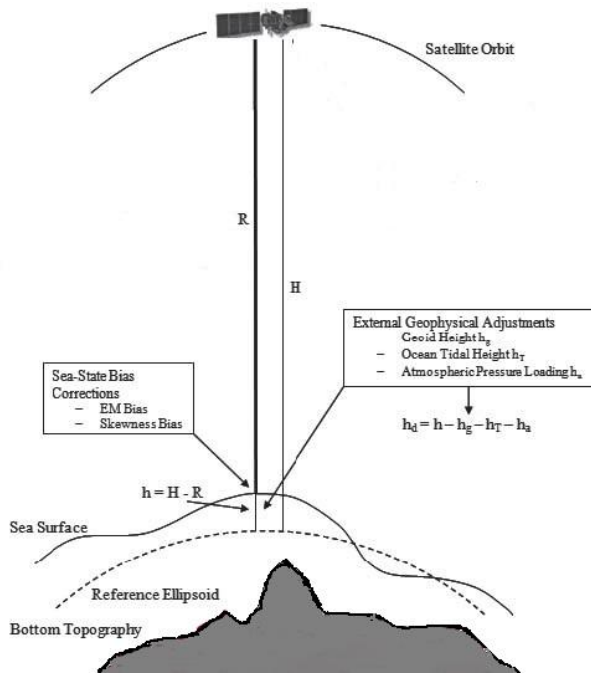
Figure 3. An illustration of height measurement using satellite Altimetry
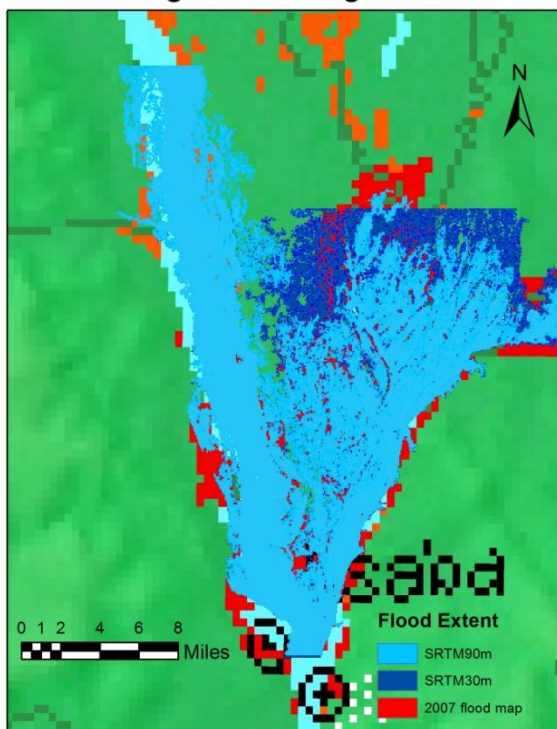

Figure 4. Model simulation result of flooding on the Niger River (2007) using SRTM topographic data